Permeation of PEO-PBLA-FITC Polymeric Micelles in Aortic Endothelial Cells

Jiahorng Liaw,[1,4] Takao Aoyagi,[2] Kazunori Kataoka,[3] Yasuhisa Sakurai,[2] and Teruo Okano[2]

Received August 15, 1998; accepted October 15, 1998

Purpose. To determine aortic endothelial cells permeation ability and mechanisms of the aqueous block copolymeric micelles, poly(ethylene oxide)-poly (β-benzyl L-aspartate) (PEO-PBLA) chemically conjugated with fluroescein isothiocyanate (FITC) by transport study and confocal laser scanning microscopy.

Methods. The block copolymers' PEO-PBLA-FITC was first synthesized and characterized by gel permeation chromatography (GPC) reflect index, UV, fluorescence detectors, and critical micelles concentrations (CMC), and atomic force microscopy (AFM). Permeation ability and mechanisms of polymeric micelles in aortic endothelial cells were evaluated by incubating with NaF, NaN_3, wortmannin, cytochalasin B inhibitors, at 20°C, and under reverse conditions. FITC and latex particles (40 nm) were also used for comparison of transport ability. The extent of localization of uptake polymeric micelles was established by confocal laser scanning microscopy.

Results. The size of the aqueous PEO-PBLA-FITC polymeric micelles was detected at around 56 nm with unimodal distribution by AFM. The CMC test revealed the fluorescence intensity increased to around 0.01 ~ 0.05 mg/ml. NaF, NaN_3, wortmannin, cytochalasin B, 20°C, and reverse experiments inhibited the absorption of polymeric micelles through aortic endothelial cells with apparent permeability coefficients (P) of 18.07 ± 1.03 to 12.98 ± 0.93, 11.31 ± 0.77, 12.44 ± 1.23, 6.40 ± 0.23, 11.11 ± 0.46, and 10.22 ± 1.09 × 10^{-7} cm/sec, respectively. Also, the permeation of FITC and latex on aortic endothelial cells was 70.02 ± 4.71, and 2.05 ± 0.41 × 10^{-7} cm/sec, respectively. Confocal laser microscopy showed that fluorescent compounds were distributed in the intracellular cytoplasm and nucleus.

Conclusions. PEO-PBLA-FITC copolymeric micelles in an aqueous system were transported by energy-dependent endocytosis with 18.07 × 10^{-7} cm/sec penetrated range and were localized on intracellular and nucleus endothelial cells.

KEY WORDS: polymeric micelles; FITC; endothelial; endocytosis.

INTRODUCTION

The selective delivery of anticancer drugs to non-operable tumors via drug carriers is one approach to rationale drug therapy (1–4). These drug delivery systems, including many different drug carriers (e.g., monoclonal antibodies, soluble polymers, liposomes, and polymeric microspheres), are often directed-attack epitopes present on tumor cells and carry drugs which interfere with tumor cells. Usually, these macromolecular carriers have to cross the tumor blood vessel wall consisting of endothelial cells and a basement membrane which are a major barriers for effective delivery (5). However, it is now accepted because of the activation of the kinin-generating cascade and the secretion of vascular permeability factor, blood capillaries at tumorous tissues develop at a considerably higher density with enhanced permeability due to the loose interendothelial junctions (6). This process leads to an enhanced passive transport of macromolecular substances, such as proteins and polymeric drugs, across the blood vessel into the interstitial spaces of the tumorous tissues.

Polymeric micelles, one of several macromolecular delivery carriers, are made from adriamycin-conjugated block copolymer PEO-PBLA (7) for selective drug delivery and have a reported high *in vivo* anticancer activity against leukemia and solid tumors as well as form stable micelles in the presence of serum and circulate in the blood stream for a long amount of time (half life $t_{1/2}$ = 6 ~ 7 h). However, the preventive transport ability between PEO-PBLA polymeric micelles and aortic endothelial membranes could depend on many parameters such as opsonic factors, the size and surface potential of the particle (8), and the composition of the particles (9). More recently, a number of studies have demonstrated the "stealth" behavior of decreased uptake by the reticuloendothelial system following the coating of particles with poly(ethylene glycol) (4,8–10), poloxamer, poloxamine, and poly(ethylene oxide) (11–12). In order to effectively utilize this character of the long circulation of polymeric micelles in the blood stream, understanding the transport ability of PEO-PBLA polymeric micelles in the aortic endothelial membrane may be essential. Thus, the purpose of the present study was to elucidate the nano range of polymeric micelles penetration mechanisms and their ability in bovine aortic endothelial cells, cultured *in vitro* as monolayers, by chemically using conjugated FITC with PEO-PBLA polymeric micelles (Fig. 1). In addition, the study aimed at determining the localization of PEO-PBLA-FITC polymeric micelles in the aortic endothelial cells by using confocal laser scanning microscopy.

MATERIALS AND METHODS

The block polymer used PEO and PBLA number average molecular weights of 12,000 g/mol and 15 unit of PBLA, respectively and was synthesized in detail elsewhere (7). Spectra/Pro dialysis membranes (Cellulose, molecular weight cutoff 3500) were obtained from Spectrum (Houston, Texas, USA). Disposable ultrafiltration units were obtained from Millipore (Bedford, Massachusetts, USA). NaF, NaN_3, wortmannin, and cytochalasin B used were from Sigma Chemical Co., (Milwaukee, Wisconsin, USA). FITC and Hoeschst 33342 (Molecular Probes Inc., Eugene, Oregon, USA) were obtained commercially. Hank's buffer solution was purchased from Gibco BRL. (Grand Island, New York, USA). All other chemicals were either reagent or analytical grade and were used as received.

Synthesis and Preparation of Aqueous Micelle-Forming PEO-PBLA with FITC Block Copolymer

Chemical conjugation and purification of PEO-PBLA with FITC moiety at chain end was done following the procedures

[1] Department of Pharmaceutics, School of Pharmacy, Taipei Medical College, Taipei, Taiwan.

[2] Institute of Biomedical Engineering, Tokyo Women's Medical University, 8-1 Kawada cho, Shinjuku, Tokyo 162, Japan.

[3] Department of Material Science, Graduate School of Engineering, The University of Tokyo, 7-3-1 Hongo, Bunkyo-ku, Tokyo 113, Japan.

[4] To whom correspondence should be addressed. (e-mail: jhorng@tmc.edu.tw)

0724-8741/99/0200-0213$16.00/0

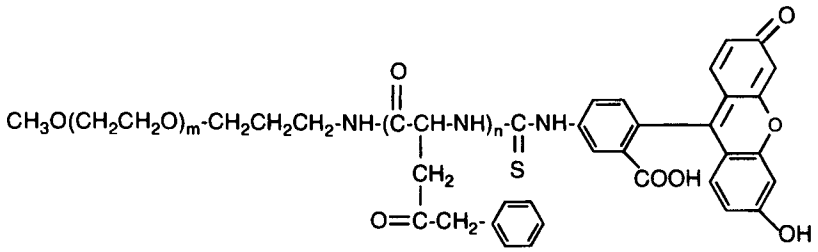

Fig. 1. The chemical structure of PEO-PBLA-FITC. PEO = 12,000 g/mol, n = 15 units.

from our previous study (13) as was the prepartion of aqueous dispersions of the PEO-PBLA-FITC copolymeric micelles. Hank's buffer solution was used to give a final concentration in the range of 0.1 mg/L to 1 mg/ml. Data for aqueous GPC were derived from preparative runs on a column of TSK gel G3000sw (30 cm × 7.8 mm). Samples (100 μl) were loaded and eluted at 1 ml/min with double distilled water. Peaks were detected using a refractive index (830RI, Jasco, Japan), UV (970UV, Jasco, Japan) and fluorescence detectors (FS8020, Tosoh, Japan).

Determination of the Critical Micelle Concentration (CMC) of PEO-PBLA-FITC Micelles

The fluorescence emission spectra of FITC were obtained using a fluorometer (FP-770, Jasco, Japan). Experiments with aqueous PEO-PBLA-FITC micelles were done with excitation and emission wavelengths of 499 and 520 nm, respectively. The calibration quantity of fluorescence emission of FITC was examined in PEO-PBLA-FITC micellar solution with a concentration range from 0.1 mg/L to 1 mg/ml. The excitation band width was set up as 5 nm and the emission band width as 3 nm. All fluorescence experiments were carried out at 25°C.

Atomic Force Microscopy Measurement

The micelle-forming PEO-PBLA-FITC (0.5 mg/ml) was applied in amounts of 1 to 2 μl on the mica surface without any treatment as in the previous study (13). The AFM used in this study was manufactured by Nanoscope III (Digital Instruments, USA) and was operated in the constant tapping mode. All images shown are raw experimental data subjected only to the normal image processing of leveling, unless otherwise specified.

Aortic Endothelial Cell Culture

Aortic endothelia cells were isolated by the method of Liu *et al.* (14). Cells were used from passage 6 up to passage 20, at a density of 5×10^5 cells/ml cell culture inserted on a Falcon 3090 poly(ethylene terephthalate) (PET) membrane (0.4 μm; Becton & Dickinson Labware, Franklin Lakes, New Jersey) with 6-well tissue culture plates (Falcon 3502). Endothelial cell monolayers were used in a complete culture medium composed of Dulbecco's modified Eagle medium (DMEM 31600; Gibco, Grand Island, New York, USA), penicillin (100 μg/ml), streptomycin (100 μg/ml), and 10% fetal bovine serum (FBS) (Gibco, Grand Island, New York, USA) within 7–14 days postseeding and were verified by direct phase contrast microscopy. The integrity of the monolayer was controlled by measuring the electrophysiological resistance. Further culturing of cells was performed as follows: (1) on cover slips of the confocal laser scanning microscopy, and (2) in vertical polymeric micelles transport.

Polymeric Micelles-PEO-PBLA-FITC Permeation Studies

The permeation of polymer micelles was determined according to a previous description by Liaw *et al.* (15). All transport experiments were performed in Hank's buffer solution at the basolateral and apical side of the monolayer and were incubated at 37°C or 20°C and 95% relative air humidity. A sample was taken at regular intervals from the receiver side, and the concentration of fluorescence was measured with a calibration curve as previously described. The apparent permeability coefficient (P) was calculated according to the following equation:

$$P = (V/A) \times (dC/dt) \times Co$$

where $V \times (dC/dt)$ is the steady-state rate of appearance of the apically applied polymeric micelles in the receiver chamber after initial lag time; Co is the initial polymeric micelles concentration in the donor chamber; and A is the area of the endothelial cells on the PET membrane. Percent permeation of transepithelial transport was calculated by comparing the amount of polymer micelles transported in the receiver chamber during a 2 h incubation.

Confocal Laser Scanning Microscopy

Cells grown on coverslips were incubated with 0.5 mg/ml PEO-PBLA-FITC polymeric micelles for 15 min and then washed with Hank's buffer solution 3 times. Thereafter the cells were scanned as vertical optical sections using a Zeiss MC 40 (Carl Zeiss Co., Oberkochen, Germany) specially modified to accommodate both an Argon and HeNe laser. Images were obtained with a Zeiss Achroplan 40× water immersion lens with a numerical aperture of 1.40. FITC was excited with the 488 nm line of the Argon laser and Hoeschst 33342 with the 350 nm band. FITC fluorescence was detected using 515/30 nm band pass filter and Hoeschst 33342 with 461/30 nm. Photoshop (Adobe System Inc., California, USA) was used for reproduction of the micrograph.

Electrical Resistance Measurement

In all experiments, two electrodes were placed on the upper and the lower chamber sides. All resistances were directly

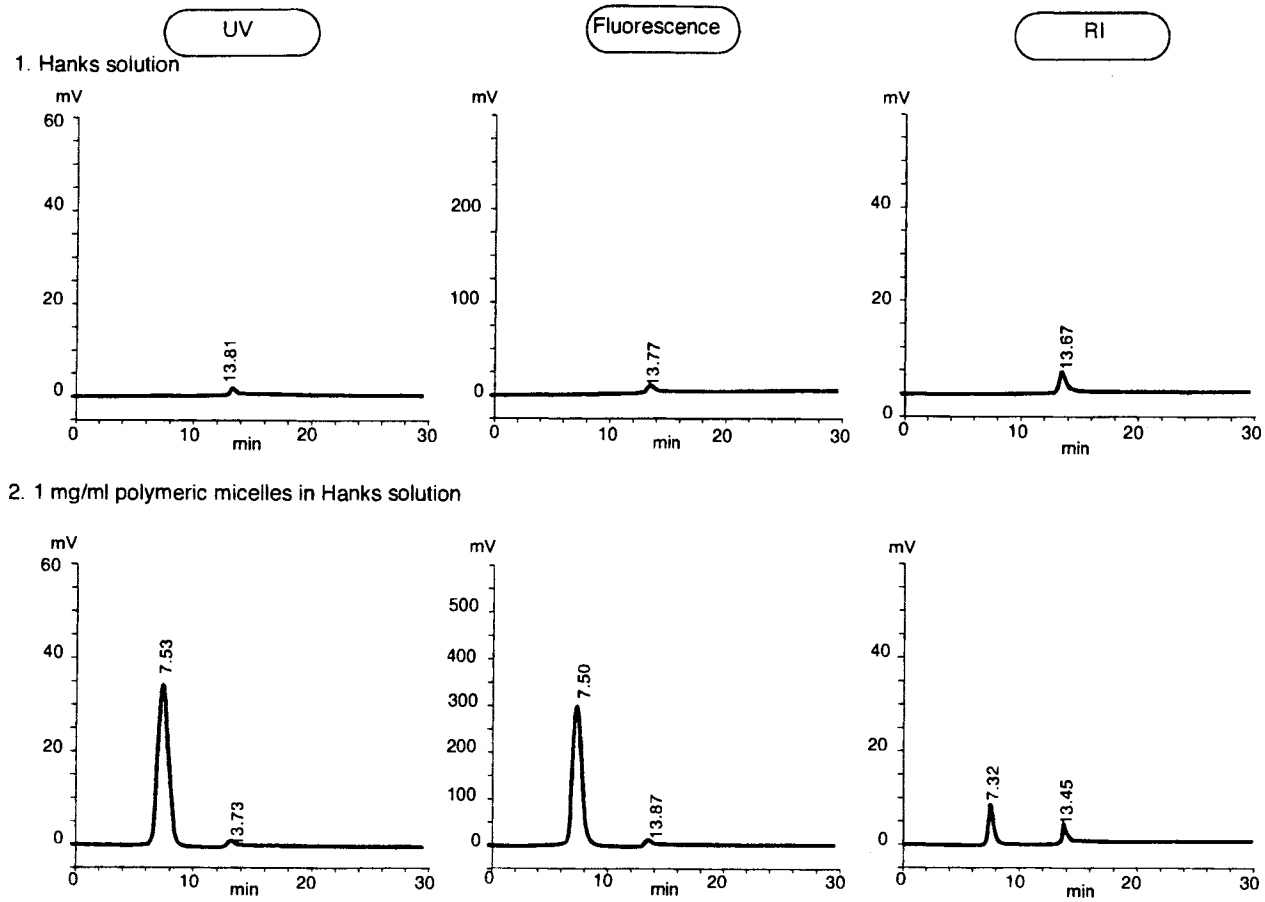

Fig. 2. Chromatograms of gel permeation chromatography of PEO-PBLA-FITC polymeric micelles in Hank's buffer solution. Peaks were detected by UV, fluorescence, and RI, using 50 μl injections of 2 mg/ml of polymeric micelles solutions with double distilled water for the mobile phase at a flow rate of 1 ml/min.

read from the Millicell-ERS resistance system (Millipore Co., Bedford, Massachusetts, USA). To correct for the potential drop due to solution resistance between the sensing electrodes and the PET membrane, measurements were carried out for each PET membrane resistance determination using the same bathing solution in the transport chamber. The actual endothelial cells resistance were then calculated by subtracting the resistance determined in the absence of the endothelial cells from that in its presence.

Statistical Methods

Results are presented as means ± standard erron mean (SEM). Statistical comparisons were made with student's *t*-test at a 99% confidence level. Differences between the tissue permeation of PEO-PBLA-FITC polymeric micelles was considered statistically significant at $p < 0.01$.

RESULTS

Characterization of PEO-PBLA-FITC Polymeric Micelles

The conjugation methods of PEO-PBLA-FITC were similar to these in a previous study (13) and subsequently the methanol and DMSO dialyzing procedures for purification of the PEO-PBLA-FITC polymers were similar as well. Micelle formations of PEO-PBLA-FITC in Hank's buffer solution are shown in Fig. 2, using 3 detectors. The molecular weight (first peak with retention time around 7.5 min) corresponding to the gel-exclusion volume is much higher than the molecular weight of this conjugate (ca. 15,000), indicating micelle formation of the conjugate. In addition, the intensity of the FITC fluorescence compound was higher than UV and RI could detect. The second peak, with retention time around 13.7 min, was influenced by the composition of Hank's buffer solution. In the meantime, the micelle-forming of PEO-PBLA-FITC solutions was tested with an RP-18 Lichrosphere column (5 μm with endcapped 250-4 mm, E. Merck Co., Darmstadt, Germany) using double distilled water for the mobile phase at a flow rate of 1 ml/min. The peaks were detected by both refractive index (ERC-7515A, ERC Inc., Japan) and UV (Spectra100, Spectra-physics, Japan) with a wave length of 280 nm. The purification results of PEO-PBLA-FITC micellar solution only showed 1 peak and a retention time was around 11 min on the charts with void volume at 1.8 min (data not shown).

The total fluorescence intensity increases of a fluorescent probe upon micellization have been utilized to determine CMC for a host of surfactants and for PEO-PS, PEO-PBLA. Figure 3 illustrates the plotting of total fluorescence intensity as a function of the logarithm of PEO-PBLA-FITC concentration.

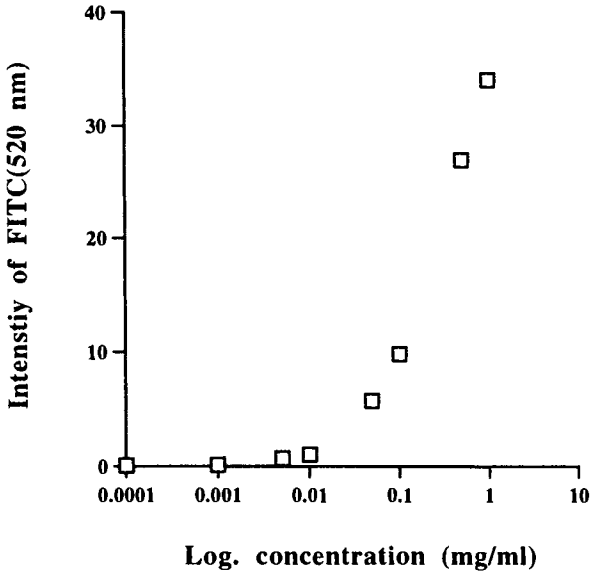

Fig. 3. Total fluorescence intensity of FITC emission versus the logarithm of PEO-PBLA-FITC concentration.

At low concentrations of PEO-PBLA-FITC (below 0.01 mg/ml), negligible changes in the total fluorescence intensity were observed. All the polymeric micelles solution permeations, and AFM and confocal microscopic measurements were carried out to at least above the CMC of the polymers.

In order to visualize the morphology of polymeric micelles, AFM was used and the polymeric micelles readily attached to the surface of mica and remained sufficiently tightly bound as imaged with an AFM tip (Fig. 4). The shape of polymeric micelles was typically observed as single, smooth, and round. The average diameter of polymeric micelles measured from one edge across the center to the other edge was found to be 56 ± 9 nm.

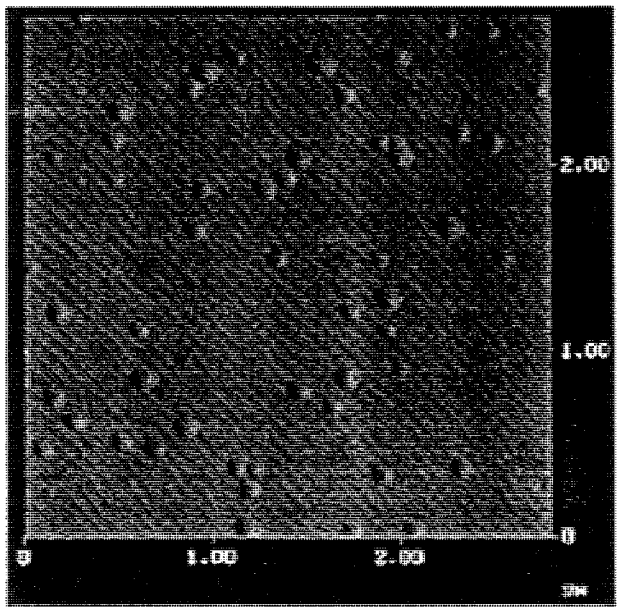

Fig. 4. AFM images of 0.1 mg/ml PEO-PBLA-FITC polymeric micelles on mica surfaces.

Permeation of PEO-PBLA-FITC Polymeric Micelles on Aortic Endothelial Cells

The time-transport profile of 0.5 mg/ml PEO-PBLA-FITC polymeric micelles across aortic endothelial monolayers in Hank's buffer solution is shown in Fig. 5. After 120 min, about 4% of the initial amount of PEO-PBLA-FITC polymeric micelles in the donor chamber had arrived in the receiver chamber. Table 1 shows that 0.05–0.5 mg/ml polymeric micelles transport through the aortic endothelial monolayer and apparent permeability coefficients were (18.89 ± 1.60, 15.05 ± 1.90, and 18.07 ± 1.03) × 10^{-7} cm/sec, respectively. It was shown that the transport properties were statistically independent of the initial concentration. Without endothelial monolayers on cell culture insert (PET membrane), polymeric micelles penetration rate increased around 10 times (P = 173.90 ± 7.07 × 10^{-7} cm/sec). It is known the action of NaF affects cell function, including the depletion of adenosine triphosphate (ATP), activation of guanosine 5′-triphosphate (GTP)-binding proteins, and mediation of the phagocytosis of components of complement C3 (17–18). Adding 5 mM NaF with polymeric micelles to endothelial cells caused the permeability to be inhibited to 12.98 ± 0.93 × 10^{-7} cm/sec. In addition, NaN_3, a blocker of oxidative phosphorylation (19), induced a similar reduction (P = 11.31 ± 0.77 × 10^{-7} cm/sec) in the transport of polymeric micelles as in the case of NaF (Table 1). Third, 100 nm wortmannin, an inhibitor of phosphatidylinostiol 3-kinase for endocytosis (20–21), inhibited 32% permeation (P = 12.44 ± 1.23 × 10^{-7} cm/sec) as well as reduced 65% penetration (P = 6.40 ± 0.23 × 10^{-7} cm/sec) by 0.1 mM cytochalasin B, an actin inhibitor. In order to confirm the energy requirement of polymeric micelles transport, diffusion studies were conducted at a temperature of around 20°C. Indeed, the uptake and influx PEO-PBLA-FITC polymeric micelles significantly decreased (P = 11.11 ± 0.46 × 10^{-7} cm/sec) as compared to the control group (37°C). In the reverse permeation studies (receiver to donor chamber), there was a marked asymmetry in the two unidirectional fluxes of polymeric micelles across the endothelial cells (P = 10.22 ± 1.09 vs. 18.07 ± 1.03 × 10^{-7} cm/sec). However, the transport of polymeric micelles in the presence of both chambers of 10% FBS serum did not influence the

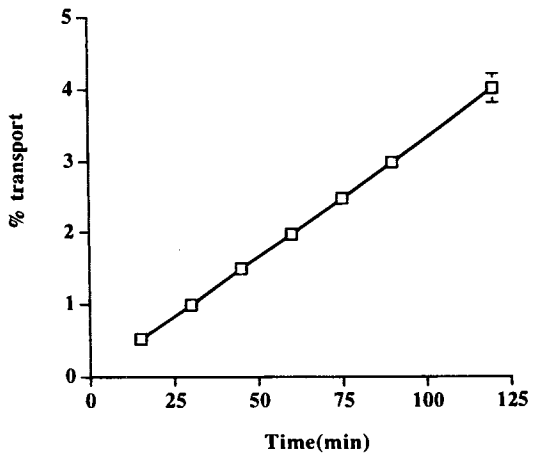

Fig. 5. Time course of PEO-PBLA-FITC polymeric micelles transport through cultured monolayers of aortic endothelial cells. Error bars represent SEM; n = 5.

Table 1. Polymeric Micelles PEO-PBLA-FITC Transport and Electrical Resistance on Aortic Endothelial Monolayers

	Apparent permeability coefficient, P ± SEM (10^7 cm/sec), (n = 5)	Endothelial electrical resistance ($\Omega.cm^2$)[a]	
		Before	After (mean ± SEM, n = 5)
1. control (without cells)[b]	173.90 ± 7.07		
control (with cells)		28 ± 8	30 ± 12
2. 0.05 mg/ml polymeric micelles[c]	18.89 ± 1.60	28 ± 12	31 ± 6
0.1 mg/ml polymeric micelles[c]	15.05 ± 1.90	32 ± 11	27 ± 6
0.5 mg/ml polymeric micelles[c]	18.07 ± 1.03	30 ± 15	42 ± 20
3. 0.5 mg/ml + 5 mM NaF[d]	12.98 ± 0.93[i]	28 ± 13	30 ± 9
4. 0.5 mg/ml + 5 mM NaN_3[d]	11.31 ± 0.77[i]	22 ± 10	24 ± 15
5. 0.5 mg/ml + 100 nM wortmannin[d]	12.44 ± 1.23[i]	27 ± 5	30 ± 11
6. 0.5 mg/ml + 0.1 mM cytochalasin B[d]	6.40 ± 0.23[i]	30 ± 7	27 ± 8
7. 0.5 mg/ml + 20°C temperature[e]	11.11 ± 0.46[i]	31 ± 6	32 ± 10
8. 0.5 mg/ml reverse effect[f]	10.22 ± 1.09[i]	35 ± 9	34 ± 6
9. 0.5 mg/ml + 10% serum[g]	18.75 ± 2.14	32 ± 10	32 ± 7
10. FITC (without cells)	202.50 ± 13.70		
FITC (with cells)	70.02 ± 4.71[i]	23 ± 7	28 ± 9
11. fluosphere (without cells)	199.10 ± 19.40		
fluosphere (with cells)[h]	2.05 ± 0.41[i]	27 ± 11	30 ± 12

[a] Electrical resistances of endothelial cells were measured at the beginning (before) and at the end (after - 2 h) of each testing condition.
[b] "Without cells" means only the cell culture was inserted (PET membrane) with 0.5 mg/ml polymeric micelles in Hanks' buffer solution.
[c] Different concentration of polymeric micelles in Hank's buffer solution through aortic endothelial cells.
[d] NaF, NaN_3, wortmannin, and cytochalasin B were incubated with 0.5 mg/ml of polymeric micelles in the donor bathing medium chamber.
[e] Transport studies were performed with a 20°C pre-equivalent incubator.
[f] Reverse effect: 0.5 mg/ml polymeric micelles were incubated in the receiver bathing medium chamber.
[g] Both sides of the bathing solution had 10% FBS added to it.
[h] Fluosphere was used with carboxylated modification (particel size = 0.04 μm).
[i] Statistical comparisons were made with student *t*-test at a 99% confidence level. Difference between the tissue uptake of 0.5 mg/ml PEO-PBLA-FITC polymeric micelles and other test condition was considered statistically significant at $p < 0.01$.

apparent permeability coefficients of polymeric micelles (P = 18.75 ± 2.14 × 10^{-7} cm/sec) through the aortic endothelial monolayers.

To compare the permselectivity of size or charge by aortic endothelial cells, two compounds: FITC and negative charge of latex, were studied as shown in Table 1. With a small molecule of FITC, molecular weight 389 Da, transport ability on the endothelial monolayer was increased to 70.02 ± 4.71 × 10^{-7} cm/sec, almost 4 times higher than that for polymeric micelles. Furthermore, the carboxylated-modified microspheres (fluospheres) have a 40 nm particle size range; the apparent permeability coefficients were found to be 2.05 ± 0.41 × 10^{-7} cm/sec and are statistically slower than 0.5 mg/ml polymeric micelles. On the other hand, FITC and fluospheres only move through the PET membrane of cell culture insert; it was found to be similar to polymeric micelles through only the cell culture insert.

Membrane resistance indicates membrane permeability, thus, it was used as an indication of tissue integrity or damage. At the end of each experiment resistances were determined at 37°C (Table 1). It can be seen at the beginning and the end of the experiments the resistance showed no significant difference when compared to tissue incubated in Hank's buffer solution.

Localization of PEO-PBLA-FITC Polymeric Micelles on Aortic Endothelial Cells by Confocal Laser Scanning Microscopy

Fifteen minutes after incubation of 0.5 mg/ml PEO-PBLA-FITC polymeric micelles in confocal laser scanning microscopy, FITC (red color) was found to be distributed over the intracellular space area, primarily at parts of endothelial monolayer cells with cytoplasm (Fig. 6a). The distributions were numerous and due to this, their close proximity, and their small particle size (around 50 nm), they were difficult to resolve individually in fluorescent microscopy. Simultaneous imaging of FITC and nuclear-live stain Hoeschst 33342 (green color) showed the majority of FITC was located around the cytoplasm and nucleus (Fig. 6b), but not between adjacent intercellular spaces. In a vertical cross-section FITC fluorescence could only be found distributed inside cells, but not on top of cells.

DISCUSSION

As the concentration of PEO-PBLA-FITC was increased, at a certain polymer concentration (ca. 0.01 mg/ml), the total fluorescence intensity in the emission spectrum (520 nm) increased dramatically in a sigmoidal manner. Similar results were seen in a previous study (13) as well as compared to the polydispersity (1.45), narrow size distribution (54.8 nm) by dyanmic light scattering, and morphology of polymeric micelles by AFM (Fig. 4). These are in agreement with the closed association of single polymer chains into micelles (7).

Before elucidating the permeation and interaction mechanisms of PEO polymeric micelles through endothelial cells, it is necessary to confirm the cell culture system such as transport ability. First, Mizuguchi *et al.* (22) used three markers, sucrose and FITC-dextran 4400, and 71200, as paracellular transport to compare the primary endothelial cell culture transport system. They found permeability coefficients of sucrose, FITC-dextran

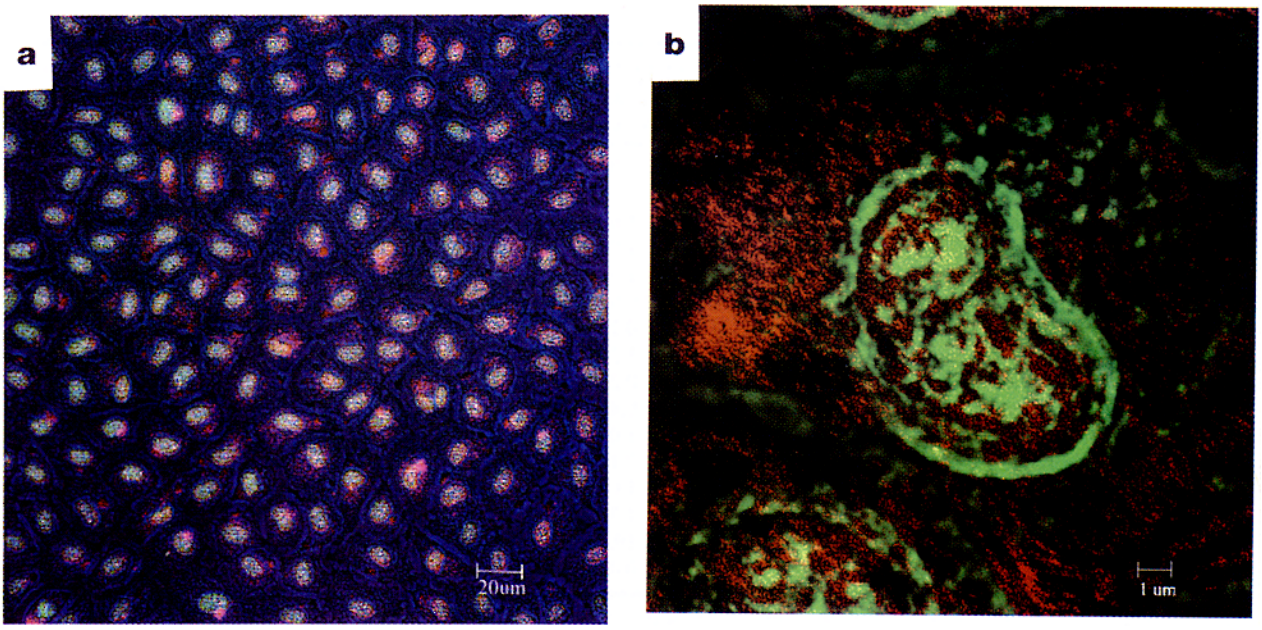

Fig. 6. Transport of 0.5 mg/ml PEO-PBLA-FITC polymeric micelles across the aortic endothelial cell monolayer for 15 min by confocal fluorescence microscopy. (a) FITC transport (red) were stained in the cytoplasm and nucleus. Live nucleus-staining by Hoeschst 33342 (green) was observed in the nucleus. Bar = 20 μm. (b) A closer look inside the cytoplasm, and some FITC (red) can also be observed in the nucleus area. Bar = 1 μm.

4400 and 71200 through bovine endothelial cells were sequentially decreased, 191 ± 10, 15.9 ± 2.7, and 4.41 ± 0.69 × 10^{-7} cm/sec, respectively. Our permeation of FITC data through aortic endothelial cells fell in between the range of permeation of sucrose and FITC-dextran 4400. Second, Gillies *et al.* (23) reported the electrical resistance measurement of aortic endothelial cells was 34.8 ± 6.8 Ω.cm^2, a similar value compared with our resistance data (Table 1). However, Rutten *et al.* (24) also found aortic endothelial cells had a smaller value (13.5 ± 0.2 Ω.cm^2) and they mentioned that with an *in vivo* system, the permeation value is 1 order smaller than the *in vitro* system due to the rapid loss of some enzyme activities e.g., alkaline phosphatase and r-glutamyl transpeptidase (r-GTP). Taking together permeation and resistance data, suggests our transport system could fall in the range and maintain cell integrity and function.

It is known polymeric micelles, having hydrophilic PEO chains as palisade regions, have been found to prohibit cellular interaction, avoid liver uptake, and while long circulating in the blood stream, but it is unclear as to the permeation ability of PEO-PBLA-FITC polymeric micelles with the normal physiological condition. First, it can be seen that after incubation of the polymeric micelles nanospheres with 10% FBS serum by endothelial cells (Table 1), permeation ability was not significantly reduced compared to values obtained in the absence of serum. Dunn *et al.* (9) reported poly(lactide-co-glycolide) (PGLA) particle uptake was significantly reduced by coating Poloxamer polymers in the presence of serum. They suggested that this may be due to a greater thickness of the adsorbed layer or becuase the longer the PEO chain of polymer on polystyrene, or PGLA nanospheres, the lower the phagocytic index and the lesser extent of particle-cell interaction. Our results was consistent with their experimental results as well as those reported by Waltrous-Peltier *et al.* (25).

Regarding surface charge of particle, a significant reduction in the percentage transport was seen after incubation with carboxylated-modified fluosphere (40 nm). The surface charge-zeta potential of polymeric micelles PEO-PBLA-FITC was around the 0 mV range vs. the negative charge of the fluospheres. Jani *et al.* (26) have also demonstrated uptake of non-ionized polystyrene nanoparticles was greater than the uptake of negatively charged (carboxylated) particles by the rat GI membrane. In addition, fluospheres and polymeric micelles move through only PET membranes of cell insert dishes with similar values and thus, the main difference between fluospheres and polymeric micelles could be due to the surface charge or composition of polymer particles.

To understand transport mechanisms of polymeric micelles on endothelial cells, some inhibitors, lower temperature, and reverse experiments were examined. Polymeric micelles transport as determined by apparent permeability coefficients was significantly more effective at 37°C than at 20°C, which may indicate the importance of cell metabolism for polymeric micelles. The permeation at 20°C was not further decreased by NaN_3 or NaF or wortmannin, suggesting polymeric micelles were already at equilibrium and could not be further inhibited by suppressing ATP metabolism. Simultaneous addition of two of three inhibitors led to almost the same reduction of permeability as did NaF alone. These results demonstrated polymeric micelles penetration was not totally inhibited by suppressing ATP-generation. A spontaneous, non-energy-driven process like membrane fusion, insertion into the membrane, or some other mechanisms by polymeric micelles are, therefore, most likely to play a role.

Whereas NaF, NaN_3, and wortmannin affect cells by interfering with ATP-metabolism, cytochalasin B acts selectively as an actin inhibitor, and the participation of cytoskeletal elements, actin filaments, and tight junction controllers in cellular

motility processes such as membrane invaginations (18–19), is well known. Thus, the penetration ability of 0.1 mM cytochalasin B with polymeric micelles was decreased to 35% and indicated that cytochalasin B inhibited the phagocytosis of polymeric micelles on aortic endothelial cells. From the *in vitro* results presented here, it is clear a combination of different mechanisms plays a role in aortic endothelial cells penetration of polymeric micelles. In general, the uptake of particles is believed to be mediated by the nonspecific association (or adsorption) of particles (liposomes, microparticles) onto the cell surface and subsequent endocytosis. Using 3 different concentrations of polymeric micelles incubated in aortic endothelial cells, the permeation ability did not show a significant difference. However, this may be due to the concentration range not being wide enough for examination. Furthermore, our reversed unidirectional transport ability studies on endothelial cells showed a different transport mechanism or transport binding protein (27) is involved in different sites of endothelial cell . However, the real binding mechanism still needs to be further examined.

Although the surface of polymeric micelles of PEO-PBLA-FITC contained the PEO group, which might invaginate membrane fusion agent, in our microscopy and confocal laser microscopy (Fig. 6a), we did not observe the fusion phenomenon after incubation with polymeric micelles. Also, we incubated FITC in the aortic endothelial monolayers and observed a major distribution of FITC in the paracellular area (data not shown). Finally, the simultaneous imaging of PEO-PBLA-FITC transport and the live nuclear-staining Hoeschst 33342 made it possible to obtain insights into the mechanisms of transport. The present confocal laser microscopy visualization studies indicate a major location of this high molecular weight particle is in the cytoplasm and nucleus and we can exclude the paracellular pathway. However, due to the nano range of this particle, there are some limits for our observation by confocal laser microscopy whether each polymeric micelles particle or single polymer is transported or diffuses into the cytoplasm. In addition, after collecting from receiver chamber, it is not easy to identify single polymer or polymeric micelles by limitation of GPC method due to small amount of transport and dynamic movement of polymeric micelles inside of the cell or receiver chamber environments.

In conclusion, PEO-PBLA-FITC a major transport route, 15 minutes after incubation, was intracellular and located in the cytoplasm and nucleus. The present four studies with 3 inhibitors, cytochalasin B, low temperature, and reverse conditions indicated that PEO-PBLA-FITC polymeric micelles permeation was unidirectional, and polymeric micelles transport appeared to involve endocytosis and some energy requirement in the permeability range of 18.07×10^{-7} cm/sec.

ACKNOWLEDGMENTS

The authors wish to thank Drs. A. Kikuchi, K. Suzuki, H. Shirakawa, and Mrs. M. Saito for their technical help and fruitful discussions. This work was partially supported by a grant from the National Science Center (NSC88-2314-B038-104).

REFERENCES

1. G. Molema, L. F. H. de Leij, and D. K. F. Meijer. Tumor vascular endothelium: barrier or target in tumor directed drug delivery and immunotherapy. *Pharm. Res.* **14**:2–10 (1997).
2. M. Yokoyama, M. Miyauchi, N. Yamada, Y. Okano, Y. Sakurai, K. Kataoka, and S. Inoue. Characterization and anticancer activity of the micelles-forming polymeric anticancer drug adriamycin-conjugated poly(ethylene glycerol)-poly(aspartic acid) block copolymer. *Cancer Res.* **50**:1693–1700 (1990).
3. F. C. Mooren, A. Berthold, W. Domschke, and J. Kreuter. Influence of chitosan microspheres on the transport of prednisolone sodium phosphate across HT 29 cell monolayers. *Pharm. Res.* **15**:58–65 (1998).
4. A. Vertut-Doi, H. Ishiwata, and K. Miyajima. Binding and uptake of liposomes containing a poly(ethylene glycol) derivative of cholesterol (stealth liposome) by the macrophage cell line J774: influence of PEG content and its molecular weight. *Bioch. Biophys. Acta.* **1278**:19–28 (1996).
5. H. Lum and A. B. Malik. Regulation of vascular endothelial barrier function. *Am. J. Physiol.* **267**:L223–241 (1994).
6. H. Maeda, L. W. Seymour, and Y. Miyamoto. Conjugates of anticancer agents and polymers: advantages of macromolecular therapeutics in vivo. *Bioconjugate Chem.* **3**:351–361 (1992).
7. G. S. Kwon, M. Naito, M. Yokoyama, T. Okano, Y. Sakurai, and K. Kataoka. Physical entrapment of adriamycin in AB block copolymer micelles. *Pharm. Res.* **12**:192–195 (1995).
8. F. X. Lacasee, M. C. Fillion, N. C. Phillips, E. Escher, J. N. McMullen, and P. Hildgen. Influence of surface properties at biodegradable microsphere surfaces: effects on plasma protein adsorption and phagocytosis. *Pharm. Res.* **15**:312–317 (1998).
9. J. S. Hrkach, M. T. Peracchia, A. Domb, N. Lotan, and R. Langer. Nanotechnology for biomaterials engineering: structural characterization of amphiphilic polymeric nanoparticles by 1H NMR spectroscopy. *Biomaterials* **18**:27–30 (1997)
10. S. Zalipsky. Chemistry of polyethylene glycol conjugates with biologically active molecules. *Adv. Drug Del. Rev.* **16**:157–182 (1995).
11. S. E. Dunn, A. G. A. Coombes, M. C. Garnett, S. S. Davis, M. C. Davies, and L Illum. *In vitro* cell interaction and in vivo biodistribution of poly(lactide-co-glycolide) nanospheres surface modified by poloxamer and poloxamine copolymers. *J. Contr. Rel.* **44**:65–76 (1997).
12. V. P. Torchilin. Polymer-coated long-circulating microparticulate pharmaceuticals. *J. Microencapsulation* **15**:1–19 (1998).
13. J. Liaw, T. Aoyagi, K. Kataoka, Y. Sakurai, and T. Okano. Visualization of PEO-PBLA-Pyene polymeric micelles by atomic force microscopy. *Pharm. Res.* **15**:1721–1726 (1998).
14. S. M. Liu, K. E. Magnusson, and T. Sundqvust. Microtubules are involved in transport of macromolecules by vesicles in cultured bovine aortic endothelial cells. *J. Cellular Physiol.* **156**:311–316 (1993).
15. J. Liaw, and J. R. Robinson. The effect of polyethylene glycol molecular weight on corneal transport and the related influence of penetration enhancers. *Int. J. Pharm.* **88**:125–140 (1992).
16. R. E. Ratych, R. S. Chuknyiska, and G. B. Bulkley. The primary localization of free radical generation after anoxia/reoxygenation in isolated endothelial cells. *Surgery* **102**:122–131 (1987).
17. K. Okada and E. J. Brown. Sodium fluoride reveals multiple pathways for regulation of surface expression of the C3b/C4b receptor (CR1) on human polymorphonuclear leukocytes. *J. Immunol.* **140**:878–884 (1988).
18. K. D. Lee, S. Nir, and D. Papahadjopoulos. Quantitative analysis of liposome-cell interaction in vitro; rate constants of binding and endocytosis with suspension and adherent J774 cells and human monocytosis. *Biochemistry* **32**: 889–899 (1993).
19. U. Pleyer, J. Grammer, P. Kosmidis, and D. Ruckert. Analysis of interactions between the corneal epithelium and liposomes: qualitative and quantitative fluorescence studies of a corneal epithelial cell line. *Surv. Ophthalmol.* **39**:S3–S16 (1995).
20. J. L. Martys, C. Wjasow, D. M. Gang, M. C. Kielian, T. E. McGraw, and J. M. Backer. Wortmannin-sensitive trafficking pathways in Chinese hamster ovary cells. *J. Biol. Chem.* **27**:10953–10962 (1996).
21. N. Ninomiya, K. Hazeki, Y. Fukui, T. Seya, T. Okada, O. Hazeki, and M. Ui. Involvement of phosphatidylinositol 3-kinase in Fcr receptor signaling. *J. Biol. Chem.* **269**:22732–22737 (1994).

22. H. Mizuguchi, Y. Hashika, N. Utoguchi, K. Kubo, S. Nakagawa, and T. Mayumi. A comparison of drug transport through cultured monolayers of bovine brain capillary and bovine aortic endothelial cells. *Biol. Pharm. Bull.* **17**:1385–1390 (1994).
23. M. C. Gillies, T. Su, and D. Naidoo. Electrical resistance and macromolecular permeability of retinal capillary endothelial cells. *Current Eye Res.* **14**:435–442 (1995).
24. M. J. Rutten, R. L. Hoover, and M. J. Karnovsky. Electrical resistance and macromolecular permeability of brain endothelial monolayer cultures. *Brain Research* **425**:301–310 (1987).
25. N. Waltrous-Peltier, J. Uhl, V. Steel, L. Brophy, and E. Merisko-Liversidge. Direct suppression of phagocytosis by amphipathic polymeric surfactants. *Pharm. Res.* **9**:1177–1183 (1992).
26. P. Jani, G. W. Halber, J. Langridge, and A. T. Florence. The uptake and translocation of latex nanospheres and microspheres after oral administration to rats. *J. Pharm. Pharmcol.* **41**:809–812 (1989).
27. D. W. Miller, E. V. Batrakova, T. O. Waltner, V. Y. Alakhov, and A. V. Kabanov. Interationsof plluronic block copolymers with brain microvessel endothelial cells: evidence of two potential pathways for drug absorption. *Bioconjugate Chem.* **8**:649–657 (1997).